Soft Matter

ARTICLE TYPE

Cite this: DOI: 00.0000/xxxxxxxxxx

Destructive effect of fluctuations on the performance of a Brownian gyrator †

Pascal Viot,[a‡] Aykut Argun,[b‡], Giovanni Volpe, [b‡],Alberto Imparato [c‡], Lamberto Rondoni [d‡], and Gleb Oshanin[a‡]

Received Date
Accepted Date

DOI: 00.0000/xxxxxxxxxx

[a] *Sorbonne Université, CNRS, Laboratoire de Physique Théorique de la Matière Condensée (UMR CNRS 7600), 4 Place Jussieu, 75252 Paris Cedex 05, France. Email: pascal.viot@sorbonne-universite.fr*
[b] *Physics Department, University of Gothenburg, 412 96 Gothenburg Sweden*
[c] *Department of Physics and Astronomy, University of Aarhus, Ny Munkegade, Building 1520, DK–8000 Aarhus C, Denmark*
[d] *Dipartimento di Scienze Matematiche, Politecnico di Torino, Corso Duca degli Abruzzi 24, 10129 Torino, Italy*
† Electronic Supplementary Information (ESI) available: [details of any supplementary information available should be included here]. See DOI: 00.0000/00000000.
‡ 'These authors contributed equally to this work.

1 Electronic Supplementary Information

1.1 Standard continuous-time BG model and the position probability density function

In the standard settings [1,2], the BG model is defined by a pair of coupled overdamped continuous-time Langevin equations of the form

$$\begin{aligned} \dot{X}_t &= -X_t + uY_t + \xi_x(t)\,, \\ \dot{Y}_t &= -Y_t + uX_t + \xi_y(t)\,, \end{aligned} \tag{S1}$$

where t is a continuous time variable, the dot denotes the time-derivative, the coupling parameter $|u| < 1$, while $\xi_x(t)$ and $\xi_y(t)$ are independent Gaussian noises with zero mean and the covariance function

$$\overline{\xi_i(t)\xi_j(t')} = 2T_j\delta_{i,j}\delta(t-t')\,, \quad i,j = x,y\,. \tag{S2}$$

As in eqs. (4) and (12) presented in the main text, in eqs. (S2) the overbar denotes averaging over realisations of noises $\xi_{x,y}(t)$, while $\delta_{i,j}$ and $\delta(t)$ are the Kronecker symbol and the delta-function, respectively. For $u = 0$, eqs. (S1) and (S2) describe two independent Ornstein-Uhlenbeck processes.

The solutions of eqs. (S1) with the initial conditions $X_0 = Y_0 = 0$ and $\dot{X}_0 = \dot{Y}_0 = 0$ are explicitly given by

$$\begin{aligned} X_t &= e^{-t}\int_0^t d\tau\, e^{\tau}\cosh\left(u(t-\tau)\right)\,\xi_x(\tau) + e^{-t}\int_0^t d\tau\, e^{\tau}\sinh\left(u(t-\tau)\right)\,\xi_y(\tau)\,, \\ Y_t &= e^{-t}\int_0^t d\tau\, e^{\tau}\sinh\left(u(t-\tau)\right)\,\xi_x(\tau) + e^{-t}\int_0^t d\tau\, e^{\tau}\cosh\left(u(t-\tau)\right)\,\xi_y(\tau)\,. \end{aligned} \tag{S3}$$

We focus next on the characteristic function

$$\phi(\nu_1,\nu_2) = \overline{\exp\left(i\nu_1 X_t + i\nu_2 Y_t\right)}\,. \tag{S4}$$

The averaging in the latter expression can be performed straightforwardly to give

$$\phi(\nu_1,\nu_2) = \exp\left(-T_x\int_0^t d\tau\, Q_x^2(t,\tau) - T_y\int_0^t d\tau\, Q_y^2(t,\tau)\right)\,, \tag{S5}$$

where

$$\begin{aligned} Q_x(t,\tau) &= e^{-(t-\tau)}\Big(\nu_1\cosh\left(u(t-\tau)\right) + \nu_2\sinh\left(u(t-\tau)\right)\Big)\,, \\ Q_y(t,\tau) &= e^{-(t-\tau)}\Big(\nu_1\sinh\left(u(t-\tau)\right) + \nu_2\cosh\left(u(t-\tau)\right)\Big)\,. \end{aligned} \tag{S6}$$

Performing the integrals in eqs. (S6), we find

$$T_x\int_0^t d\tau\, Q_x^2(t,\tau) + T_y\int_0^t d\tau\, Q_y^2(t,\tau) = a\nu_1^2 + b\nu_2^2 - c\nu_1\nu_2\,, \tag{S7}$$

where we have used the shortenings

$$a = \frac{T_x p + T_y q}{4(1-u^2)}\,, \quad b = \frac{T_x q + T_y p}{4(1-u^2)}\,, \quad c = \frac{(T_x+T_y)\,l}{2(1-u^2)}\,, \tag{S8}$$

with

$$\begin{aligned} p &= 2 - u^2 - e^{-2t}\Big(\cosh\left(2ut\right) + u\sinh\left(2ut\right)\Big) - (1-u^2)e^{-2t}\,, \\ q &= u^2 - e^{-2t}\Big(\cosh\left(2ut\right) + u\sinh\left(2ut\right)\Big) + (1-u^2)e^{-2t}\,, \\ l &= u - e^{-2t}\Big(u\cosh\left(2ut\right) + \sinh\left(2ut\right)\Big)\,. \end{aligned} \tag{S9}$$

Having defined the characteristic function, we find eventually the position probability density function by merely inverting the Fourier

transform:

$$P(X_t,Y_t) = \frac{1}{(2\pi)^2}\int_{-\infty}^{\infty}\int_{-\infty}^{\infty} d\nu_1\, d\nu_2\, e^{-i\nu_1 X_t - i\nu_2 Y_t}\,\phi(\nu_1,\nu_2)$$
$$= \frac{1}{2\pi d}\exp\left(-\frac{bX_t^2 + aY_t^2 + cX_tY_t}{d^2}\right), \tag{S10}$$

where $d = \sqrt{4ab-c^2}$ and the coefficients a, b and c are defined in eqs. (S8) and (S9). Note that the solution for a somewhat more general model with arbitrary coefficients in eqs. (S1) is also available[3–5].

1.2 Probability density function of the specific angular momentum

1.2.1 Characteristic function $\Phi_{\mathscr{L}}(\nu)$.

We focus here on the characteristic function of the specific angular momentum which is formally defined by

$$\Phi_{\mathscr{L}}(\nu) = \overline{\exp\left(i\nu\mathscr{L}\right)}. \tag{S11}$$

Using the formal definition of $\mathscr{L}$ in eq. (2) and the discrete-time evolution equations eq. (1) we have

$$\mathscr{L} = u\left(X_t^2 - Y_t^2\right) + \sqrt{\frac{2T_y}{\delta t}}\,X_t\,\eta_y(t) - \sqrt{\frac{2T_x}{\delta t}}\,Y_t\,\eta_x(t), \tag{S12}$$

such that the characteristic function of the specific angular momentum reads

$$\Phi_{\mathscr{L}}(\nu) = \overline{\exp\left(i\nu u\left(X_t^2 - Y_t^2\right) + i\nu\sqrt{\frac{2T_y}{\delta t}}\,X_t\eta_y(t) - i\nu\sqrt{\frac{2T_x}{\delta t}}\,Y_t\eta_x(t)\right)}. \tag{S13}$$

In virtue of eq. (1) the components X_t and Y_t of the BG position at time instant t are statistically-independent of the values of noises at this very time instant. Therefore, we can average the latter expression with respect to $\eta_x(t)$ and $\eta_y(t)$. In doing so, we get

$$\Phi_{\mathscr{L}}(\nu) = \overline{\exp\left(-\left(\frac{T_y}{\delta t}\,\nu^2 - i\nu u\right)X_t^2 - \left(\frac{T_x}{\delta t}\,\nu^2 + i\nu u\right)Y_t^2\right)}, \tag{S14}$$

which yields, upon averaging with the PDF in eq. (S10), the following explicit result:

$$\Phi_{\mathscr{L}}(\nu) = \left(1 - 4i(a-b)u\,\nu + 4\left(\frac{bT_x + aT_y}{\delta t} + u^2d^2\right)\nu^2 - 4iud^2\,\frac{(T_x - T_y)}{\delta t}\,\nu^3 + 4d^2\,\frac{T_xT_y}{\delta t^2}\,\nu^4\right)^{-1/2}, \tag{S15}$$

where the coefficients a, b and c are defined in eqs. (S8) and (S9), and $d = \sqrt{4ab-c^2}$. Therefore, the characteristic function $\Phi_{\mathscr{L}}(\nu)$ is the inverse of a square-root of a quartic polynomial of ν and becomes ill-defined, as mentioned above, in the limit $\delta t \to 0$. In the limit $t \to \infty$, the expression (S15) attains the form

$$\Phi_{\mathscr{L}}(\nu) = \left(1 - 2iu\,(T_x - T_y)\,\nu + \frac{(1+u^2\delta t)\left(4T_xT_y + u^2(T_x-T_y)^2\right)}{(1-u^2)\delta t}\,\nu^2\right.$$
$$\left. - i\,\frac{u(T_x-T_y)\left(4T_xT_y + u^2(T_x-T_y)^2\right)}{(1-u^2)\delta t}\,\nu^3 + \frac{T_xT_y\left(4T_xT_y + u^2(T_x-T_y)^2\right)}{(1-u^2)\delta t^2}\,\nu^4\right)^{-1/2}. \tag{S16}$$

The above expression permits us to access the usual properties characterising the probability density function, i.e., the moments and the cumulants. In particular, differentiating eq. (S16) with respect to ν once and twice, and setting $\nu = 0$ afterwards, we find explicit expressions for the first moment and the variance of $\mathscr{L}$ in eqs. (8) and (9).

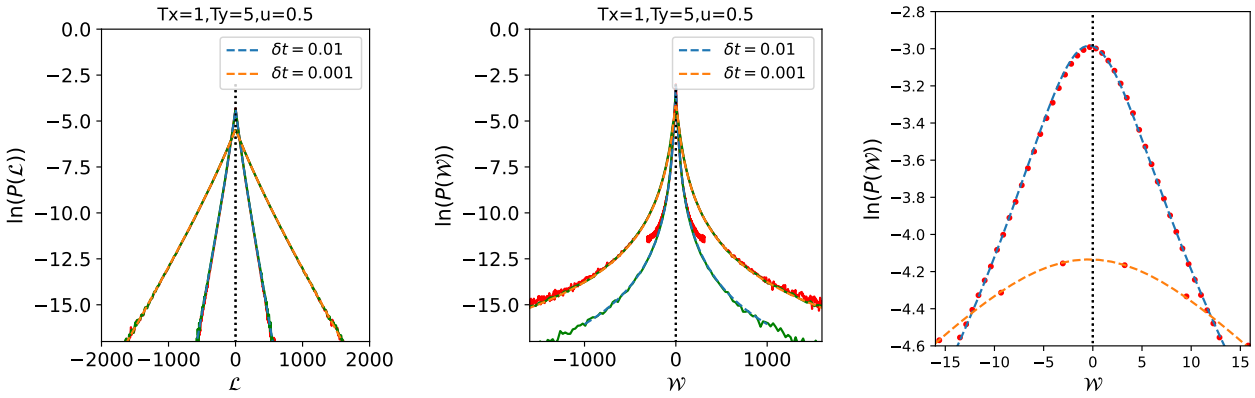

Fig. S1 Comparison of theoretical predictions for the probability density functions in eqs. (4) and (12) and the results of numerical simulations for two values of the time-step δt: $\delta t = 0.01$ (blue) and $\delta t = 0.001$ (magenta); and fixed $T_x = 1$, $T_y = 5$ and $u = 0.5$. Left panel: Logarithm of $P(\mathscr{L})$ versus $\mathscr{L}$. Dashed curves correspond to the exact expression, eq. (4), whereas the noisy curves depict the simulation results obtained using the approaches I and II (see below). Central panel: Logarithm of $P(\mathscr{W})$ versus $\mathscr{W}$. Dashed curves depict the exact expression, eq. (12), and the noisy curves - the simulation results. Right panel: Zoom of the region around the maximal value of $P(\mathscr{W})$. Dashed curves are theoretical predictions in eq. (12). while the symbols indicate the results of numerical simulations.

1.2.2 Probability density function $P(\mathscr{L})$.

The probability density function of the specific angular momentum is formally defined as

$$P(\mathscr{L}) = \frac{1}{2\pi}\int_{-\infty}^{\infty}\int_{-\infty}^{\infty} dX_t\, dY_t\, P(X_t,Y_t)\int_{-\infty}^{\infty} d\nu\, \exp\left(-i\nu\mathscr{L} - \left(\frac{T_y}{\delta t}\nu^2 - i\nu u\right)X_t^2 - \left(\frac{T_x}{\delta t}\nu^2 + i\nu u\right)Y_t^2\right)$$
$$= \sqrt{\frac{\delta t}{4\pi}}\int_{-\infty}^{\infty}\int_{-\infty}^{\infty}\frac{dX_t\, dY_t}{\sqrt{T_y X_t^2 + T_x Y_t^2}} P(X_t,Y_t)\,\exp\left(-\frac{\delta t\left(\mathscr{L} - u\left(X_t^2 - Y_t^2\right)\right)^2}{4\left(T_y X_t^2 + T_x Y_t^2\right)}\right). \tag{S17}$$

Turning to polar coordinates through the transformation $X_t = \rho\cos(\theta)$ and $Y_t = \rho\sin(\theta)$, we formally rewrite the expression in the second line in eq. (S17) as

$$P(\mathscr{L}) = \frac{1}{2d}\sqrt{\frac{\delta t}{\pi}}\int_0^{2\pi}\frac{d\theta}{\sqrt{T_y\cos^2(\theta) + T_x\sin^2(\theta)}}\int_0^{\infty} d\rho\,\exp\left(-\frac{\delta t\left(\mathscr{L} - u\rho^2\cos(2\theta)\right)^2}{4\rho^2(T_y\cos^2(\theta) + T_x\sin^2(\theta))}\right)$$
$$\times\exp\left(-\left(\frac{b\cos^2(\theta) + a\sin^2(\theta) + c\cos(\theta)\sin(\theta)}{d^2}\right)\rho^2\right). \tag{S18}$$

Performing the integral over ρ, we find the expression (4). In Fig. S1 (left panel) we present a comparison between our theoretical prediction for $P(\mathscr{L})$ in eq. (4) and the results of numerical simulations. One observes a perfect agreement.

1.2.3 Finite δt. Large-$\mathscr{L}$ asymptotic behaviour of $P(\mathscr{L})$.

The function $\Xi(\theta)$, eq. (5),is an oscillatory function of the polar angle θ, which has two minima (and two maxima) of equal depth (height) on the interval $[0, 2\pi]$ (see Fig. S2). In general, the minima corresponding to $\mathscr{L} > 0$ and $\mathscr{L} < 0$ are attained at somewhat different values of θ and have somewhat different depths, which signifies that $P(\mathscr{L})$ is asymmetric around $\mathscr{L} = 0$. In the limit $\mathscr{L} \to \infty$, the integral in eq. (4) is entirely dominated by the behavior of Ξ in the close vicinity of the minima, which yields the exponential asymptotic form in eq. (10). Differentiating $\Xi(\theta)$ with respect to θ and equating the resulting expression to zero, we find an equation that determines the positions of the extrema of Ξ. This is a fourth-order algebraic equation whose solution has a rather cumbersome form. We therefore consider only the limiting case when the coupling parameter u is close (but not equal) to zero and δt is also small, in which limit it is possible to present rather compact explicit results. A rather cumbersome but straightforward analysis shows that here

$$\frac{1}{L_\pm} = \sqrt{\frac{\delta t}{2T_xT_y}}\left(1 - \frac{(T_y + T_x)}{2\sqrt{T_xT_y}}|u| + O\left(u^2\right)\right). \tag{S19}$$

When $u = 0$, we recover from the latter expression the result in eq. (7).

Another situation, in which a systematic analysis of the large-$\mathscr{L}$ asymptotic behaviour is possible, is that of thermodynamic equilibrium, i.e., $T_x = T_y = T$. Here, we pursue a slightly different approach focusing on the characteristic function in eq. (S16), which becomes

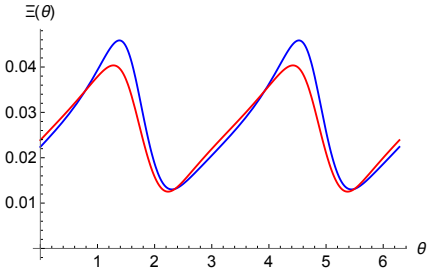

Fig. S2 The function $\Xi(\theta)$ in eq. (5) versus the polar angle θ for $T_x = 1$, $T_y = 5$, $u = 1/2$ and $\delta t = 0.1$. Red solid curve corresponds to $\mathscr{L} > 0$, while the blue one - to $\mathscr{L} < 0$.

(for $u^2 \delta t \ll 1$)

$$\Phi_{\mathscr{L}}(v) = \left(1 + \frac{4T^2}{(1-u^2)\delta t}\, v^2 + \frac{4T^4}{(1-u^2)\delta t^2}\, v^4\right)^{-1/2}. \tag{S20}$$

The latter expression can be formally rewritten as

$$\begin{aligned} \Phi_{\mathscr{L}}(v) &= \frac{\sqrt{(1-u^2)}}{\sqrt{\left(1 + \dfrac{2T^2 v^2}{\delta t}\right)^2 - u^2}} \\ &= \sqrt{(1-u^2)} \int_0^\infty dx\, I_0(|u|x) \exp\left(-\left(1 + \frac{2T^2 v^2}{\delta t}\right) x\right), \end{aligned} \tag{S21}$$

and hence, the probability density function attains the form

$$P(\mathscr{L}) = \frac{\sqrt{(1-u^2)\delta t}}{2\sqrt{2\pi} T} \int_0^\infty \frac{dx}{\sqrt{x}} I_0(|u|x) \exp\left(-x - \frac{\delta t \mathscr{L}^2}{8T^2 x}\right), \tag{S22}$$

where I_0 is the modified Bessel function of the first kind. Setting $u = 0$ in eq. (S22), we recover our eq. (7) with $T_x = T_y = T$. Upon some inspection, we realise that the large-$\mathscr{L}$ (more precisely, $\delta t \mathscr{L}^2/(8T^2)$ is to be large and u - to be bounded away from zero) behaviour of $P(\mathscr{L})$ is supported by the large-x behaviour of the integrand. To this end, we take advantage of the Hankel's asymptotic expansion of the modified Bessel function

$$I_0(z) = \frac{e^z}{\sqrt{2\pi z}} \left(1 + \frac{1}{8z} + \frac{9}{2(8z)^2} + O\left(\frac{1}{z^3}\right)\right). \tag{S23}$$

Inserting the latter expansion into eq. (S22) and performing integrations, we arrive at the converging asymptotic large-$\mathscr{L}$ expansion of the form

$$\begin{aligned} P(\mathscr{L}) = &\left(\frac{1-u^2}{8\pi T |u\mathscr{L}|}\right)^{1/2} \left(\frac{2\delta t}{(1-|u|)}\right)^{1/4} \exp\left(-\sqrt{\frac{(1-|u|)\delta t}{2}} \frac{|\mathscr{L}|}{T}\right) \\ &\times \left(1 - \frac{(3|u|-2)T}{4\sqrt{2(1-|u|)\delta t\, |u\mathscr{L}|}} + \frac{3T^2}{16\delta u^2 \mathscr{L}^2} + O\left(\frac{1}{|\mathscr{L}|^3}\right)\right). \end{aligned} \tag{S24}$$

Consequently, we recover the asymptotic form in eq. (10) with

$$L_+ = L_- = \sqrt{\frac{2}{(1-|u|)\delta t}}\, T, \tag{S25}$$

which is fully consistent with eq. (S19). Note that the higher order terms in δt and u are evidently missing here because we assumed that $u^2 \delta t \ll 1$.

1.2.4 Continuous-time limit $\delta t \to 0$. Asymptotic behavior of $P(\mathscr{L})$.

We concentrate on the behaviour of the probability density function $P(\mathscr{L})$ in the limit $\delta t \to 0$. One notices that in this limit the second term in eq. (6) becomes much larger than the first term, (i.e., $u^2 \cos^2(2\theta)$), which can be therefore safely neglected. In consequence,

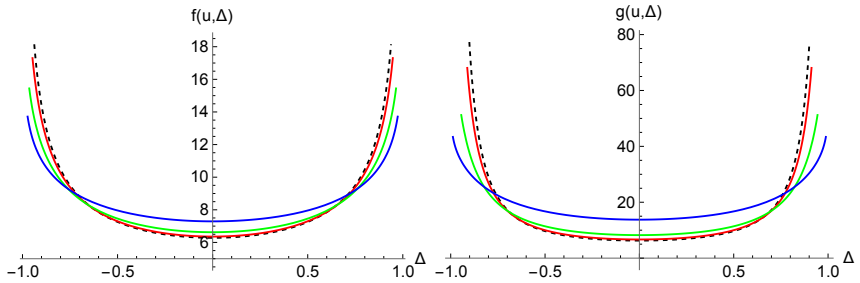

Fig. S3 Small δt limit. Left panel : $f(u,\delta)$ in eq. (S29) as function of $\Delta=(T_x-T_y)/(T_x+T_y)$. Right panel: $g(u,\delta)$ in eq. (S39) as function of Δ. In both panels the dashed curve corresponds to $u=0$, red solid curve - to $u=1/4$, green - to $u=1/2$ and blue - to $u=3/4$.

we have

$$\Lambda(\theta)\simeq\frac{2}{d\sqrt{\delta t}}\left(\left(T_x\sin^2(\theta)+T_y\cos^2(\theta)\right)\left(b\cos^2(\theta)+a\sin^2(\theta)+c\cos(\theta)\sin(\theta)\right)\right)^{1/2}, \tag{S26}$$

which implies that $\Lambda(\theta)$ diverges when $\delta t\to 0$. In this limit, the first term in the nominator in eq. (5) is much larger than the second term, (i.e., $\mathrm{sign}(\mathscr{L})u\cos(2\theta)$), which can be neglected. Therefore, the function $\Xi(\theta)$ in eq. (5) obeys (in this limit)

$$\begin{aligned}\Xi(\theta)&\simeq\frac{\Lambda(\theta)}{2\left(T_y\cos^2(\theta)+T_x\sin^2(\theta)\right)}\delta t\\&=\left(\frac{b\cos^2(\theta)+a\sin^2(\theta)+c\cos(\theta)\sin(\theta)}{T_x\sin^2(\theta)+T_y\cos^2(\theta)}\right)^{1/2}\frac{\sqrt{\delta t}}{d}\end{aligned} \tag{S27}$$

and hence, vanishes in proportion to the square-root of δt.

We assume that $t\to\infty$, in which case the coefficients a, b and c attain sufficiently simple time-independent forms. Using the definitions of the coefficients a, b and c, and conveniently rewriting the terms entering the expression (S26) as

$$\begin{aligned}&T_x\sin^2(\theta)+T_y\cos^2(\theta)=\frac{T_x+T_y}{2}\left(1-\Delta\cos(2\theta)\right),\quad \Delta=\frac{T_x-T_y}{T_x+T_y},\\&b\cos^2(\theta)+a\sin^2(\theta)+c\cos(\theta)\sin(\theta)=\frac{T_x+T_y}{4(1-u^2)}\left(1+u\sin(2\theta)-(1-u^2)\Delta\cos(2\theta)\right).\end{aligned} \tag{S28}$$

Further on, we suppose that $\mathscr{L}$ is finite (i.e., $\mathscr{L}\delta t$ is small when $\delta t\to 0$) and expand the expression in the right-hand-side of eq. (4) into the Taylor series in powers of δt. In doing so, we realise that, in the leading in the limit δt order, the probability density function $P(\mathscr{L})$ in eq. (4) is given by eq. (11) with

$$f(u,\Delta)=\int_0^{2\pi}\frac{d\phi}{\sqrt{\left(1-\Delta\cos(\phi)\right)\left(1+u\sin(\phi)-(1-u^2)\Delta\cos(\phi)\right)}}. \tag{S29}$$

The integral in the latter equation cannot be performed exactly. To get an idea of the behaviour of $f(u,\Delta)$, we depict it in Fig. S3 as function of Δ for several values of the coupling parameter u. Note that $f(u,\Delta)$ is (logarithmically) diverging in the limit $\Delta\to\pm 1$, i.e., when either of the temperatures vanishes. It was shown in[6] that this limit is rather peculiar and the case when either of the temperatures vanishes is to be treated separately. We therefore suppose that both $T_x,T_y>0$. Further on, correction terms to the leading asymptotic behaviour in eq. (11) are of order $\mathscr{L}\delta t$. We verified that the coefficient in front of $\mathscr{L}\delta t$ is finite, such that a uniform distribution of $\mathscr{L}$ in the limit $\delta t\to 0$ is a valid feature.

1.3 Probability density function of the specific angular velocity.

1.3.1 Characteristic function $\Phi_{\mathscr{W}}(\nu)$.

Using the discrete-time Langevin eq. (1), we write the specific angular velocity as

$$\mathscr{W}=\frac{u\left(X_t^2-Y_t^2\right)}{X_t^2+Y_t^2}+\frac{\sqrt{2T_y}X_t\,\eta_y(t)-\sqrt{2T_x}Y_t\,\eta_x(t)}{\sqrt{\delta t}\left(X_t^2+Y_t^2\right)}, \tag{S30}$$

such that characteristic function $\Phi_{\mathscr{W}}(\nu)$ is given by :

$$\Phi_{\mathscr{W}}(\nu) = \overline{\exp\left(i\nu u \frac{(X_t^2 - Y_t^2)}{X_t^2 + Y_t^2} + i\nu \frac{\sqrt{2T_y} X_t \, \eta_y(t) - \sqrt{2T_x} Y_t \, \eta_x(t)}{\sqrt{\delta t}\,(X_t^2 + Y_t^2)} \right)}. \tag{S31}$$

Again, noticing that the instantaneous values of the noises $\eta_x(t)$ and $\eta_y(t)$ at time t have no effect on the instantaneous positions X_t and Y_t at this very time, we straightforwardly average over $\eta_x(t)$ and $\eta_y(t)$ to get

$$\Phi_{\mathscr{W}}(\nu) = \overline{\exp\left(i\nu u \frac{(X_t^2 - Y_t^2)}{X_t^2 + Y_t^2} - \frac{T_y \nu^2 X_t^2}{\delta t (X_t^2 + Y_t^2)^2} - \frac{T_x \nu^2 Y_t^2}{\delta t (X_t^2 + Y_t^2)^2} \right)}. \tag{S32}$$

1.3.2 Probability density function $P(\mathscr{W})$.

The probability density function $P(\mathscr{W})$ of the specific angular velocity is formally defined as

$$\begin{aligned} P(\mathscr{W}) &= \frac{1}{2\pi} \int_{-\infty}^{\infty} d\nu \, \Phi_{\mathscr{W}}(\nu) \, e^{-i\nu\mathscr{W}} \\ &= \frac{1}{2\pi} \int_{-\infty}^{\infty} d\nu \, e^{-i\nu\mathscr{W}} \int_{-\infty}^{\infty}\int_{-\infty}^{\infty} dX_t \, dY_t \, P(X_t, Y_t) \\ &\times \exp\left(i\nu u \frac{(X_t^2 - Y_t^2)}{X_t^2 + Y_t^2} - \frac{T_y \nu^2 X_t^2}{\delta t (X_t^2 + Y_t^2)^2} - \frac{T_x \nu^2 Y_t^2}{\delta t (X_t^2 + Y_t^2)^2} \right). \end{aligned} \tag{S33}$$

Changing the integration variables to polar coordinates, we formally rewrite the latter expression as

$$\begin{aligned} P(\mathscr{W}) &= \frac{1}{(2\pi)^2 \sqrt{4ab - c^2}} \int_0^{2\pi} d\theta \int_{-\infty}^{\infty} d\nu \, \exp\left(i\nu \left(u\cos(2\theta) - \mathscr{W} \right) \right) \\ &\times \int_0^{\infty} \rho \, d\rho \, \exp\left(-\frac{\nu^2 \left(T_y \cos^2(\theta) + T_x \sin^2(\theta) \right)}{\delta t \rho^2} - \left(\frac{b\cos^2(\theta) + a\sin^2(\theta) + c\cos(\theta)\sin(\theta)}{4ab - c^2} \right) \rho^2 \right) \\ &= \frac{1}{\pi^2 \delta t \sqrt{4ab - c^2}} \int_0^{2\pi} \frac{(T_y \cos^2(\theta) + T_x \sin^2(\theta)) \, d\theta}{\sqrt{\Lambda^2(\theta) - u^2 \cos^2(2\theta)}} \int_0^{\infty} \nu \, d\nu \cos\left(\nu \left(u\cos(2\theta) - \mathscr{W} \right) \right) \\ &\times K_1\left(\sqrt{\Lambda^2(\theta) - u^2\cos^2(2\theta)} \, \nu \right), \end{aligned} \tag{S34}$$

where K_1 is the modified Bessel function and $\Lambda(\theta)$ is defined in eq. (6). Performing the integral over ν, we arrive at our result in eq. (12).

1.3.3 Finite δt. Large-$\mathscr{W}$ asymptotic behaviour of $P(\mathscr{W})$.

Asymptotic large-$\mathscr{W}$ behaviour of the probability density function $P(\mathscr{W})$ in eq.(12) can be accessed very directly by merely expanding the denominator in inverse powers of $\mathscr{W}$. Verifying that all the integrals defining the coefficients in this expansion exist, we find

$$P(\mathscr{W}) = \frac{(T_x + T_y)}{2d\delta t} \frac{1}{|\mathscr{W}|^3} - \frac{3u(T_x - T_y)}{4d\delta t} \frac{1}{\mathscr{W}^4} + o\left(\frac{1}{\mathscr{W}^4} \right). \tag{S35}$$

In the limit $t \to \infty$, eq. (S35) gives

$$P(\mathscr{W}) = \frac{\sqrt{1-u^2}(T_x + T_y)}{\sqrt{4T_xT_y + u^2(T_x - T_y)^2}\delta t} \frac{1}{|\mathscr{W}|^3} + \frac{3u\sqrt{1-u^2}(T_y - T_x)}{2\sqrt{4T_xT_y + u^2(T_x - T_y)^2}\delta t} \frac{1}{\mathscr{W}^4} + o\left(\frac{1}{\mathscr{W}^4} \right). \tag{S36}$$

The first term in this expansion is our eq. (14) presented in the main text, while the second term defines the sub-dominant contribution. Interestingly enough, the amplitude of the second term vanishes in equilibrium conditions (i.e., for $T_x = T_y$) such that in equilibrium the sub-dominant contribution will vanish with $\mathscr{W}$ at a faster rate.

Because of the algebraic tail, $P(\mathscr{W})$ has only the first moment. In virtue of eq. (S30), we have

$$\begin{aligned}\overline{\mathscr{W}} &= u\overline{\left(\frac{X_t^2-Y_t^2}{X_t^2+Y_t^2}\right)} = u\int_{-\infty}^{\infty}\int_{-\infty}^{\infty} dX_t dY_t\, P(X_t,Y_t)\left(\frac{X_t^2-Y_t^2}{X_t^2+Y_t^2}\right)\\ &= \frac{u\sqrt{1-u^2}(T_x-T_y)}{\sqrt{4T_xT_y+u^2(T_x-T_y)^2}}\,.\end{aligned} \tag{S37}$$

This is a well-known result which shows that $\overline{\mathscr{W}}$ is not equal to zero when simultaneously $u\neq 0$ and $T_x\neq T_y$. In general, $\overline{\mathscr{W}}$ is a non-monotonic function of the coupling constant u, which vanishes when either $u=0$ or $|u|=1$ and, hence, attains a maximal value for some intermediate coupling.

1.3.4 Continuous-time limit $\delta t\to 0$. Asymptotic behaviour of $P(\mathscr{W})$.

We focus on the PDF $P(\mathscr{W})$ defined in eq. (12) and suppose that $\mathscr{W}$ is finite. Since $\Lambda(\theta)$ diverges in the limit $\delta t\to 0$, in the leading in δt order, we are entitled to $\mathscr{W}$-dependent terms in the denominator. Then, using eqs. (S26) and (S28), we have

$$\begin{aligned}P(\mathscr{W}) &\simeq \frac{d^2\sqrt{\delta t}}{16\pi}\int_0^{2\pi}\frac{d\theta}{(T_y\cos^2(\theta)+T_x\sin^2(\theta))^{1/2}(b\cos^2(\theta)+a\sin^2(\theta)+c\cos(\theta)\sin(\theta))^{3/2}}\\ &= \frac{(4T_xT_y+u^2(T_x-T_y)^2)}{8\pi(T_x+T_y)^2}\sqrt{2(1-u^2)\delta t}\int_0^{2\pi}\frac{d\phi}{\sqrt{(1-\Delta\cos(\phi))(1+u\sin(\phi)-(1-u^2)\Delta\cos(\phi))^3}}\,,\end{aligned} \tag{S38}$$

i.e., our eq. (15) with $g(u,\Delta)$ given by

$$g(u,\Delta)=\int_0^{2\pi}\frac{d\phi}{\sqrt{(1-\Delta\cos(\phi))(1+u\sin(\phi)-(1-u^2)\Delta\cos(\phi))^3}}\,. \tag{S39}$$

Likewise $f(u,\Delta)$ in eq. (S29), $g(u,\Delta)$ diverges logarithmically when $\Delta\to\pm 1$, i.e., either of the temperatures vanishes. Therefore, the asymptotic form in eq. (15) is valid only when both temperatures are bounded away from zero.

1.3.5 Probability density function $P(\mathscr{W})$ in the decoupled case $u=0$.

Lastly, we aim to find an analogue of eq. (7) which describes the probability density function $P(\mathscr{L})$ in the decoupled case $u=0$. For $u=0$, the probability density function in eq. (12) 1becomes (in the limit $t\to\infty$)

$$P(\mathscr{W})=\frac{1}{2\pi}\sqrt{\frac{\delta t}{T_xT_y}}\int_0^{2\pi}\frac{\left(T_y\cos^2(\theta)+T_x\sin^2(\theta)\right)d\theta}{\left(\delta t\,\mathscr{W}^2+\frac{2}{T_xT_y}\left(T_y\cos^2(\theta)+T_x\sin^2(\theta)\right)^2\right)^{3/2}}\,. \tag{S40}$$

Using the first of eqs. (S28) and the integral identity

$$\frac{p}{\left(a^2+p^2\right)^{3/2}}=\int_0^{\infty}\tau\, d\tau\, J_0(a\tau)\, e^{-p\tau}\,, \tag{S41}$$

we cast eq. (S40) into the form

$$\begin{aligned}P(\mathscr{W}) &= \sqrt{\frac{\delta t}{2}}\int_0^{\infty}\tau\, d\tau J_0\left(\sqrt{\delta t}\,\mathscr{W}\tau\right)J_0\left(i\frac{(T_x+T_y)}{\sqrt{2T_xT_y}}\Delta\tau\right)\exp\left(-\frac{(T_x+T_y)}{\sqrt{2T_xT_y}}\tau\right)\\ &= -\sqrt{\frac{\delta t}{2}}\frac{d}{d\alpha}\int_0^{\infty}d\tau J_0\left(\sqrt{\delta t}\,\mathscr{W}\tau\right)J_0(i\beta\tau)\exp(-\alpha\tau)\,,\quad \alpha=\frac{(T_x+T_y)}{\sqrt{2T_xT_y}}\,,\quad \beta=\frac{(T_x-T_y)}{\sqrt{2T_xT_y}}\,.\end{aligned} \tag{S42}$$

The integral in the last line in eq. (S42) can be performed explicitly to give

$$P(\mathscr{W})=-\frac{\delta t^{1/4}}{\pi\sqrt{2i\beta\mathscr{W}}}\frac{d}{d\alpha}Q_{-1/2}\left(\frac{\alpha^2+\delta t\,\mathscr{W}^2-\beta^2}{2i\beta\mathscr{W}\sqrt{\delta t}}\right), \tag{S43}$$

where $Q_{-1/2}$ is the Legendre function. It might be also convenient to express the result in eq. (S43) in an explicit form using the Gauss hypergeometric functions:

$$P(\mathscr{W}) = \frac{(T_x+T_y)\sqrt{T_xT_y\delta t\,(2+\delta t\,\mathscr{W}^2)}}{2(2T_y+T_x\delta t\,\mathscr{W}^2)(2T_x+T_y\delta t\,\mathscr{W}^2)}\,{}_2F_1\left(3/4,1/4;1;-\frac{2(T_x-T_y)\delta t\,\mathscr{W}^2}{T_xT_y(2+\delta t\,\mathscr{W}^2)^2}\right) + \frac{(T_x-T_y)^2\delta t^{3/2}\mathscr{W}^2}{4(T_xT_y)^{3/4}(2+\delta t\,\mathscr{W}^2)^{3/2}(2T_y+T_x\delta t\,\mathscr{W}^2)(2T_x+T_y\delta t\,\mathscr{W}^2)}\,{}_2F_1\left(5/4,3/4;2;-\frac{2(T_x-T_y)\delta t\,\mathscr{W}^2}{T_xT_y(2+\delta t\,\mathscr{W}^2)^2}\right). \tag{S44}$$

Importantly, when two processes, eq. (1) are decoupled, the probability density function $P(\mathscr{W})$ is an even function of $\mathscr{W}$, such that it is symmetric around $\mathscr{W}=0$, likewise the probability density function of the angular momentum (see eq. (7)). The dependence on temperatures and the functional form of the probability density function $P(\mathscr{W})$ are evidently much more complicated than $P(\mathscr{L})$ in eq. (7).

1.4 Probability density function of the moment of inertia

We evaluate here the probability density function of the moment of inertia $\mathscr{I}=X_t^2+Y_t^2$, which is a positive definite random variable. Therefore, it is convenient to focus on its moment-generating function

$$\Phi_{\mathscr{I}}(\lambda) = \overline{\exp\left(-\lambda\mathscr{I}\right)}, \quad \lambda \geq 0, \tag{S45}$$

for which one readily obtains the following exact result

$$\Phi_{\mathscr{I}}(\lambda) = \left(1+4(a+b)\lambda+4d^2\lambda^2\right)^{-1/2}, \tag{S46}$$

where the coefficients a, b, c and d are defined in eqs. (S8) and (S9). Inverting the latter expression, we find the probability density function

$$P(\mathscr{I}) = \frac{1}{2d}\exp\left(-\frac{(a+b)}{2d^2}\mathscr{I}\right) I_0\left(\frac{\sqrt{(a-b)^2+c^2}}{2d^2}\mathscr{I}\right), \tag{S47}$$

where I_0 is the modified Bessel function. In the limit $t\to\infty$, $P(\mathscr{I})$ attains the form

$$P(\mathscr{I}) = \sqrt{\frac{1-u^2}{4T_xT_y+u^2(T_x-T_y)^2}}\exp\left(-\frac{T_x+T_y}{4T_xT_y+u^2(T_x-T_y)^2}\mathscr{I}\right) \times I_0\left(\frac{\sqrt{4u^2T_xT_y+(1-u^2+u^4)(T_x-T_y)^2}}{4T_xT_y+u^2(T_x-T_y)^2}\mathscr{I}\right). \tag{S48}$$

In the case of two decoupled Ornstein-Uhlenbeck processes (i.e., for $u=0$), the probability density function in eq. (S48) simplifies considerably to give

$$P(\mathscr{I}) = \sqrt{\frac{1}{4T_xT_y}}\exp\left(-\frac{T_x+T_y}{4T_xT_y}\mathscr{I}\right) I_0\left(\frac{|T_x-T_y|}{4T_xT_y}\mathscr{I}\right). \tag{S49}$$

In Fig. S4 the probability density function $P(\mathscr{I})$ is depicted as function of $\mathscr{I}$ for three values of u ($u=0$, 0.5 and 0.8) and temperatures $T_x=1$ and $T_y=5$. Noisy curves are the solutions of stochastic eqs. (S1) using the Euler-Maruyama algorithm, while the dot-dashed curves correspond to the analytical expression (S48). One observes a perfect agreement between the numerical results and the theoretical prediction. We also note that the most probable value of the moment of inertia $\mathscr{I}$ is attained at $\mathscr{I}=0$, which explains why large values of $\mathscr{W}$ are abundant and therefore, why $P(\mathscr{W})$ possesses heavy power-law tails.

1.5 Numerical simulations.

Numerical simulations of the BG model are performed by using the standard Euler-Maruyama algorithm. To compute the angular momentum and the angular velocity, we take advantage of two alternative approaches:
– Approach I. The first approach relies on the formal definition of $\mathscr{W}$ as the rate of change of the angular position with respect to time

$$\mathscr{W} = \frac{\delta\theta}{\delta t}, \tag{S50}$$

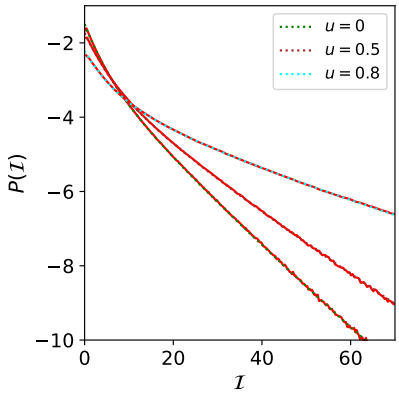

Fig. S4 The moment of inertia $\mathscr{I}$. The probability density function $P(\mathscr{I})$ versus $\mathscr{I}$ for $T_x = 1$ and $T_y = 5$. Noisy curves depict the results of numerical simulations, while dot-dashed curves - the exact expression (S48).

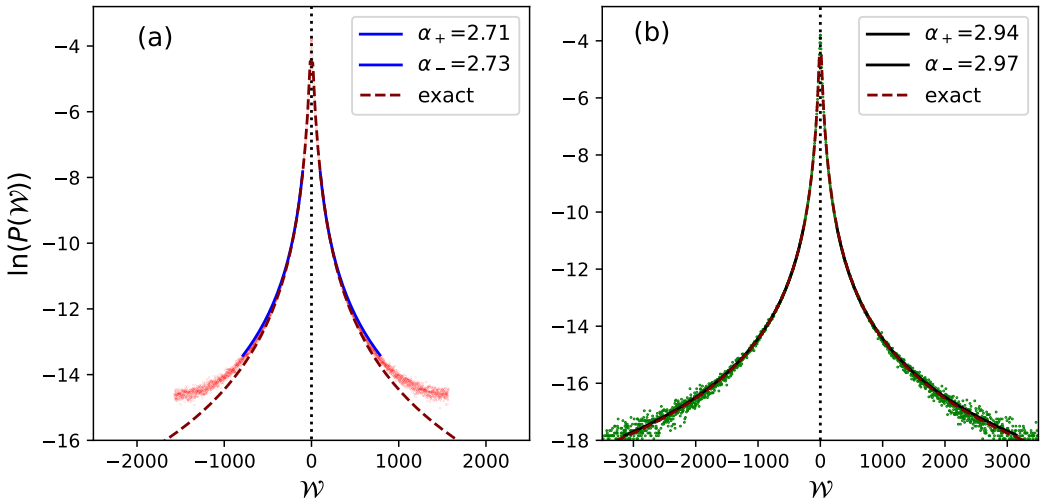

Fig. S5 Fits of the results of numerical simulations. Logarithm of the probability density function $P(\mathscr{W})$ versus $\mathscr{W}$ for $T_x = 1$, $T_y = 5$, $u = 1/2$ and $\delta t = 0.002$. The dashed curve is the exact analytical solution in eq. (12). Panel (a): The red noisy curve represents $\ln P(\mathscr{W})$ evaluated using approach I. The blue solid curves are the fits of the red curve by power-law functions $1/|\mathscr{W}|^{\alpha_-}$ for negative $\mathscr{W}$ and $1/\mathscr{W}^{\alpha_+}$ for positive $\mathscr{W}$. Panel (b): Symbols (filled green circles) depict the numerical results obtained via approach II. The solid black curves are the fits of the numerical data obtained via approach II by the above power-law functions. The inset shows the best-fit values of the exponents.

where the instantaneous value of the polar angle is expressed via the cartesian coordinates as

$$\theta = \mathrm{atan2}(Y_t, X_t) \tag{S51}$$

where the function atan2 is the 2-argument arctangent[7]. While determining $\mathscr{W}$ through eq. (S50), we exercise care that at each incremental step $\delta\theta$ does not exceed π, which is controlled by the increment δt. Note also that within this approach the distribution of the angular velocity has its support on the interval $[-\pi/\delta t, \pi/\delta t]$, so that while evaluating $P(\mathscr{W})$ we consider only such values of $\mathscr{W}$ that are away from the boundaries, in order to avoid aliasing effects appearing close to the boundaries of the interval. To access the behaviour at larger values of $\mathscr{W}$, we have to diminish the increment δt. Of course, this can be readily done in numerical simulations, but in experiments the value of δt is bounded from below by the maximal frequency at which the images of the trajectories are taken.

Once $\mathscr{W}$ is determined, the angular momentum is found via the relation

$$\mathscr{L} = (X_t^2 + Y_t^2)\mathscr{W}\,. \tag{S52}$$

Note that this approach is appropriate for the analysis of discrete-time trajectories recorded both in numerical simulations and in experiments (see Fig. (3) in the main text), because it necessitates the position data only. In Fig. S1 the results obtained using the approach I are depicted by noisy red curves.

– Approach II. The second approach hinges on the standard recursive solution of the time-discretised Langevin eq.(1), for which the

angular momentum $\mathscr{L}$ and the angular velocity $\mathscr{W}$ are determined by eqs. (S12) and (S30), respectively. Generating in numerical simulations the dimensionless noises $\eta_x(t)$ and $\eta_y(t)$, we build recursively the trajectories X_t and Y_t and eventually calculate the angular momentum and the angular velocity. Results obtained via this approach are depicted in Fig. S1 by noisy green curves. Note that this second approach is only applicable for the numerical simulations.

Lastly, we comment on the discrepancy between the theoretically predicted exponent ($=3$), characterising the tails of the probability density function $P(\mathscr{W})$, and somewhat lower values deduced from the fitting of the experimentally-evaluated PDFs. To this end, we resort to numerical simulations of the BG model using approaches I and II and preform the fitting of the numerical data, which we fully control. These fits are presented in Fig. S5. We observe that for the same value of δt (which is quite small, $\delta t = 0.002$), the PDF $P(\mathscr{W})$ obtained within the approach I is defined on a much shorter interval, as compared to the one obtained in terms of approach II, and hence, the large-$\mathscr{W}$ tails are systematically heavier than the exact solution. The best-fit values of the exponents $\alpha_\pm$ obtained within the approach I are $\alpha_- \approx 2.73$ and $\alpha_+ \approx 2.71$, respectively, which are somewhat higher that the exponents deduced from the experimental data (see Fig. 3 in the main text). This implies that the accuracy of approach I, which is used to analyzse the experimental data, can be somewhat improved by reducing δt, but the latter cannot be made arbitrarily small due to natural limits imposed on the sampling frequency of imaging the trajectories[8]. In turn, approach II appears to be more accurate giving the values of the exponents that are closer to the predicted value.

Notes and references

1 R. Exartier and L. Peliti, Phys. Lett. A, 1999, **261**, 94

2 R. Filliger and P. Reimann, Phys. Rev. Lett., 2007, **99**, 230602

3 S. Ciliberto, A. Imparato, A. Naert, and M. Tanase, Phys. Rev. Lett., 2013, **110**, 180601

4 S. Ciliberto, A. Imparato, A. Naert, and M. Tanase, J. Stat. Mech. **2013**, 12014

5 S. Cerasoli, S. Ciliberto, E. Marinari, G. Oshanin, L. Peliti, and L. Rondoni, Phys. Rev. E, 2022, **106**, 014137

6 S. Cerasoli, V. Dotsenko, G. Oshanin, and L. Rondoni, Phys. Rev. E, 2018, **98**, 042149;

7 https://en.wikipedia.org/wiki/Atan2

8 A. Argun, J. Soni, L. Dabelow, S. Bo, G. Pesce, R. Eichhorn, and G. Volpe, Phys. Rev. E, 2017, **96**, 052106